

Frying Pan Free Convection Analysis

ME 31500

Project Report

Trevor Ladner, Keegan Moster, Adam McGoff, Mark Huibregtse, Ricky Smith

December 9th, 2021

Executive Summary

The following report details an investigative study on three different materials of frying pan. In this experiment, the pans used were non-stick (aluminum with Teflon coating), stainless steel, and cast-iron; each material was chosen due to its substantial popularity throughout the cooking industry and home kitchens. Several factors were chosen to quantitatively and qualitatively evaluate each pan material. First, the steady state temperature of each pan was found to determine which pan was best for high temperatures. In addition, each pan was evaluated for how long it could maintain its steady state temperature after it was removed from the heat source. In order to minimize the heat leakage to the environment, each pan was set on an insulated block during the cooling portion of the experiment. Finally, the experimental property of the heat transfer coefficient (h) was calculated using the temperature data collected throughout the heating and cooling of each pan.

Throughout the design of the experiment, there were several technical considerations and assumptions that needed to be evaluated. Firstly, it was assumed that the wall of the pan could be treated as a rotated fin around the base of the pan, and that the pan wall was a uniform temperature throughout. In order to experimentally verify this hypothesis, a thermocouple was placed on either side of the fin in order to ensure that each temperature increased in tandem.

After testing the pans, the team was able to make several conclusions. First, it was found that the non-stick pan reached the steady state temperature the fastest. The fast-heating non-stick pan makes sense since it is largely marketed to consumers who need a fast heating solution to cook in everyday life. Additionally, the cast iron pan reached the highest steady state temperature, although it took about twice the amount of time to reach steady state. In the cooking industry, cast iron pans are often used to sear steaks and other meats since they can maintain high temperatures; our testing simply confirmed cast iron as an excellent choice for such a recipe. Finally, the stainless-steel pan was found to cool down the quickest after the heat was removed. Stainless steel pans are often used in restaurant kitchens, where pans need to be cooled quickly and washed before making another dish. The stainless-steel pan's ability to quickly cool indicated why it is so often used in the food service industry.

Table of Contents

Introduction.....	4
Experimental Model System.....	5
Analysis.....	6
Results and Discussion	9
Conclusions and Recommendations	18
References.....	20
Appendix.....	21

Introduction

The purpose of this experiment is to analyze and compare different pan materials and their properties. Each pan was evaluated at both the steady state heating and cooling case in order to determine the convection coefficient and specific heat of the material. The plan was to use empirical evidence to calculate material properties; primarily with the purpose of indicating why different pan materials are used in various cooking situations. The cookware industry is highly saturated with different materials, with many vendors claiming that their material cookware has an advantage over another. The experiment hoped to use the heat transfer coefficient to justify some of the claims made for using different materials of cookware.

The procedure for testing each pan material began by creating a test setup where the temperature of the pan and fin could be measured at multiple locations while the pan was uniformly heated. It was decided to use a coil stove to provide uniform heating properties. Thermocouples were used to measure the temperature at 12 locations across the pans. These locations can be found below in Figure 1 and Figure 2. Several adhesive options were evaluated to firmly secure the thermocouples to the pans. Thermal glue and solder were unable to firmly secure to the pan surface, and instead thermal tape was deemed to be the most suitable for the experiment. After all thermocouples were in place, the wattmeter was used to provide a voltage input of 65 Watts to the heating plate; this input was used since the temperature during all three tests needed to be consistent, and because the resultant temperature was similar to the heat a pan might actually experience while cooking on a stove. The temperature was measured using LabView until they reached steady state values. Next, the pan was moved in a manner to minimally move the heat source away from the pan and replace it with an insulated block without disturbing any of the attached thermocouples and causing any form of forced convection or unnecessary heat transfer. After the pan's transfer to the insulated block, the temperature was once again recorded until the pan reached steady state temperature. The resulting data was used to find the heat transfer coefficient of the materials, as well as indicate why different pans are recommended for different cookware situations. The main source used for the analysis and evaluation of the material properties was the course textbook, which is cited in the references section.

Experimental Model System

The schematics for experimental setup are featured below. In each experiment, the radius of the pan was considered to be 10 inches, and any heat loss through the handle was neglected. Furthermore, the pan and the fin will be analyzed separately.

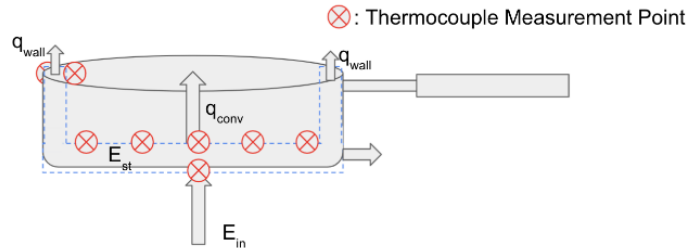


Figure 1. Lateral view of the setup for the pan. Note that in each assembly there is a thermocouple on the bottom of the pan as well as the outside of the fin to ensure that the ΔT value could be calculated across the two surfaces.

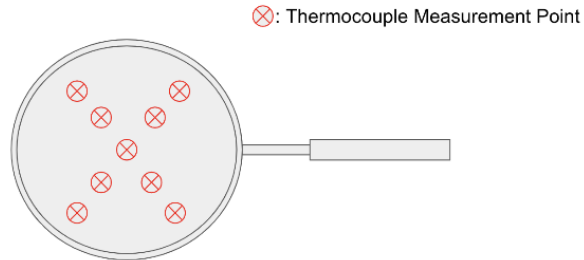


Figure 2. Medial view of the setup for the pan. Note in the assembly that the thermocouples are placed in equidistant locations outward from the center. This placement is to measure how the pan heats at varying radial distances from the center.



Figure 3. The final setup for the pan (stainless steel featured above). In this assembly, thermal tape was used to adhere each thermocouple to the pan.

Analysis

The analysis for this project can be split into two cases. The first case is the heating case, where the pan is heated from ambient temperature to a steady state temperature with a constant power input. The second case is the cooling case, where the pan is cooled from its heated steady state temperature to ambient temperature. The first part of this analysis will focus on the heating case. To start, a simple energy balance is performed on the control volume shown in Figure 1.

$$E_{in} - E_{out} + E_g = E_{st} \quad (\text{Equation 1})$$

Since there is no energy being generated within the control volume, the energy generation term cancels out. Energy terms are then substituted into the equation to yield the energy balance equation for the heating case.

$$q_{in} - q_{conv,base} - q_{conv,wall} = \left(mc_p \frac{dT}{dt} \right)_{base} + \left(mc_p \frac{dT}{dt} \right)_{wall} \quad (\text{Equation 2})$$

This equation can be further expanded by substituting in the equation for the convection terms.

$$q_{in} - \overline{h}_{base} A_{base} (T - T_{\infty}) - \overline{h}_{wall} A_{wall} (T - T_{\infty}) = \left(mc_p \frac{dT}{dt} \right)_{base} + \left(mc_p \frac{dT}{dt} \right)_{wall} \quad (\text{Equation 3})$$

The base and wall areas are defined using the following equations.

$$A_{base} = \frac{\pi}{4} D_i^2 \quad (\text{Equation 4})$$

$$A_{wall} = l_{wall} \pi D_o + l_{wall} \pi D_i \quad (\text{Equation 5})$$

Once these area expressions are substituted into Equation 3, the final form of the energy balance is obtained.

$$q_{in} - \overline{h_{base}} \left(\frac{\pi}{4} D_i^2 \right) (T - T_{\infty}) - \overline{h_{wall}} (l_{wall} \pi D_o + l_{wall} \pi D_i) (T - T_{\infty}) = \left(mc_p \frac{dT}{dt} \right)_{base} + \left(mc_p \frac{dT}{dt} \right)_{wall} \quad (\text{Equation 6})$$

After temperature data and pan dimensions are recorded, the only unknowns in Equation 6 are $\overline{h_{base}}$ and $\overline{h_{wall}}$. In order to find $\overline{h_{base}}$, empirical correlations are used. To do so, the Rayleigh number must first be calculated.

$$Ra_L = \frac{g\beta(T_s - T_{\infty})L^3}{\nu\alpha} \quad (\text{Equation 7})$$

Where this is calculated at every time in both the heating and cooling of the pans to account for the changing heat of the surrounding air and the effects that has on the buoyant forces. The value for the expansion coefficient is also found at every instant by finding the inverse of the film temperature. Next, the empirical correlations can be used to find the Nusselt number. The selected correlation is based on the calculated Rayleigh number and the position/state of the base of the pan.

$$\overline{Nu_L} = 0.54 Ra_L^{\frac{1}{4}} \quad (\text{Equation 8})$$

Lastly, the definition of the Nusselt number can be used to solve for $\overline{h_{base}}$.

$$\overline{h_{base}} = \frac{k}{L} \overline{Nu_L} \quad (\text{Equation 9})$$

Finally, once the base convection coefficient has been determined, a value for the wall convection coefficient can be calculated using the energy balance. This is done using the equation below where c_p is found for the average temperature of the pan during the process based on the material properties found in the course textbook.

$$\overline{h_{wall}} = - \frac{\overline{h_{base}} \pi D_i^2 (T_{base} - T_{\infty}) + c_p \left(m_{base} \frac{dT_{base}}{dt} + m_{wall} \frac{dT_{wall}}{dt} \right) - q_{in}}{2\pi D_i l_{wall} (T_{wall} - T_{\infty})} \quad (\text{Equation 10})$$

For the cooling case, the same process was repeated. Since the pan has now been placed on an insulated surface, there is no longer any energy input to the system. Therefore, for the cooling case, Equation 10 is used and is the same except for the fact that q_{in} is set to 0.

For each of the warming and cooling cases, a system convection coefficient was sought. This was found using the thermal mass proportions of each pan part, the base and the wall, and multiplying that by the convection coefficient for that part. Since the pan is the same material throughout, the thermal conductivity term is cancelled out. This relation be seen in Equation 11 below.

$$h_{system} = \frac{m_{base}}{m} h_{base} + \frac{m_{wall}}{m} h_{wall} \quad (Equation 11)$$

To perform this analysis, a few critical assumptions were needed. The first assumption was that the base temperature was independent of the angular position and only dependent on the radial position. This assumption simplified the model for the experiment greatly and was validated by the results. Figure 4 below shows an example of the results that allowed for this assumption from the stainless steel pan. In this plot, the temperatures are fairly similar at every time, allowing for the average temperature to be used of every point theta at that radius to inform the temperature distribution for the pan surface. Plots for the non-stick pan and cast-iron pan were similar to these.

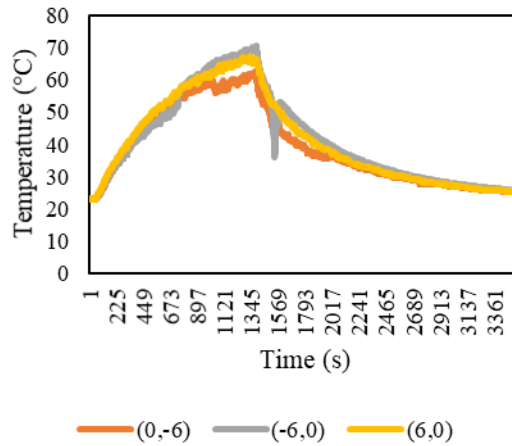


Figure 4. Temperature Plots at Various Angular Positions for the Stainless Steel Pan

The next critical assumption that had to be made was that radiation was negligible. This assumption was validated using equation 12. Using this equation, it can be determined that the radiation is at max roughly 2% of the 65W that is input into the pan for the highest pan temperature. With this in mind, it is able to be considered a negligible value in the energy balance.

$$q_{rad-max} = \sigma A_{base} T_{base}^4 \quad (Equation 12)$$

Similar to the first assumption, another assumption was that the pan wall was at uniform temperature on the interior and exterior. This was validated by using thermocouple readings from both the inside and outside as exemplified in figure 5. In this plot from the stainless steel pan, the

temperatures are very nearly identical at every time. This means that the assumption of uniform fin temperature is valid to make.

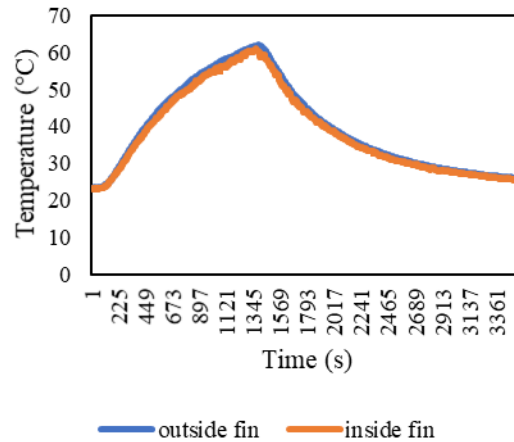


Figure 5. Fin Temperature Validation Plot

The other critical assumptions in the model were that the pans had constant thermal properties, the pan insulation was a perfect insulator, the power applied was a constant input, the handle and any contact resistance are negligible, and the wall acts as a fin and is perpendicular to the base of the pan.

Results and Discussion

At a low level, the temperature gradient at each radial point provides much information as to how each pan performed generally. Figures 6, 7, and 8 represent this. In this, the non-stick pan took the least amount of time to reach its steady state temperature. However, this temperature was lower than that of the other two pans. The cast-iron pan reached the highest steady state temperature overall. Lastly, the stainless-steel pan reached a steady state temperature near room temperature the quickest. In each of these figures, the temperature at each radial coordinate is shown. Notably, the cast iron pan appeared to have the greatest inconsistency in temperature of the surface while the non-stick pan had the most consistent temperature.

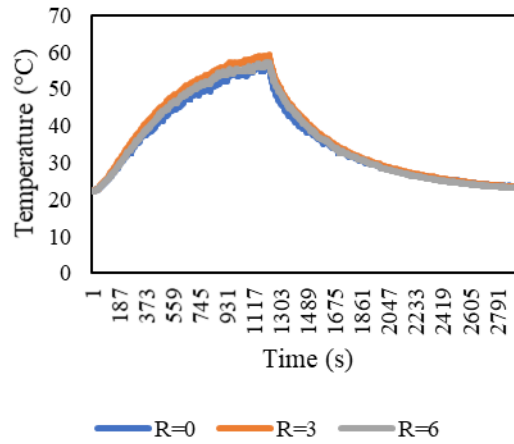


Figure 6. Temperature vs. Time for Heating and Cooling of Nonstick Pan

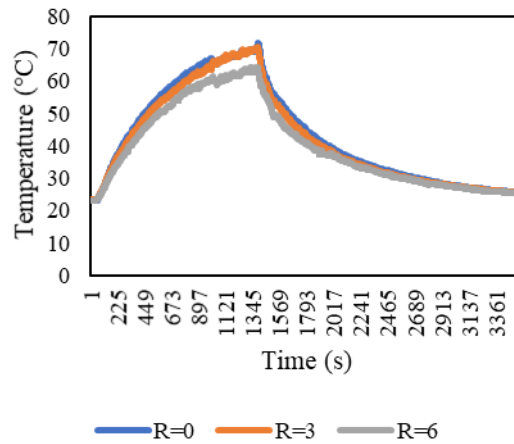


Figure 7. Temperature vs. Time for Heating and Cooling of Stainless-Steel Pan

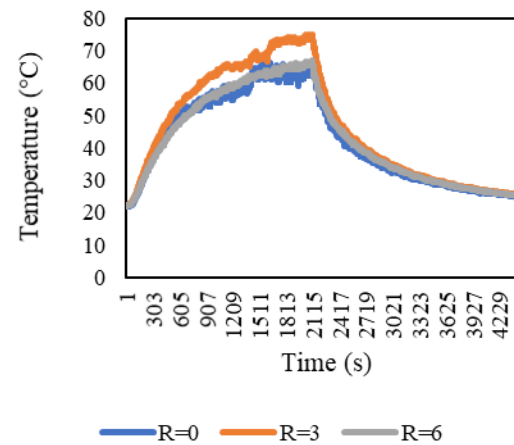


Figure 8. Temperature vs. Time for Heating and Cooling of Cast Iron Pan

The results for the convection coefficients are rather interesting. Overall, the average convection coefficient for the walls was nearly always higher than for the base of the pan. During heating, the convection coefficient was also typically much higher on the pans than during the cooling process. A breakdown of the results for the convection coefficients can be seen in the table below.

Table 1. Convection Coefficient (h) Average Values

	Stainless Steel	Non-Stick	Cast Iron
h_{base} (W/m ² *K) warming	5.9036	5.5730	7.4078
h_{wall} (W/m ² *K) warming	65.0585	25.0162	59.9906
h_{base} (W/m ² *K) cooling	4.7081	4.3553	5.1663
h_{wall} (W/m ² *K) cooling	4.5690	6.2805	10.7107

A large contributing factor to this is due to the changing Rayleigh number during the cooling and heating. The Rayleigh number relies heavily on the temperature of the surface and the film temperature. As the film temperature increases to its limit at the steady state surface temperature, the Rayleigh number also reaches a limit. This is demonstrated in figures 9 and 10.

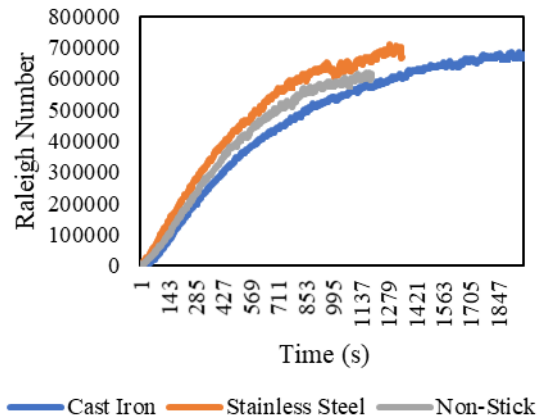


Figure 9. Rayleigh Number vs Time During Warming Process.

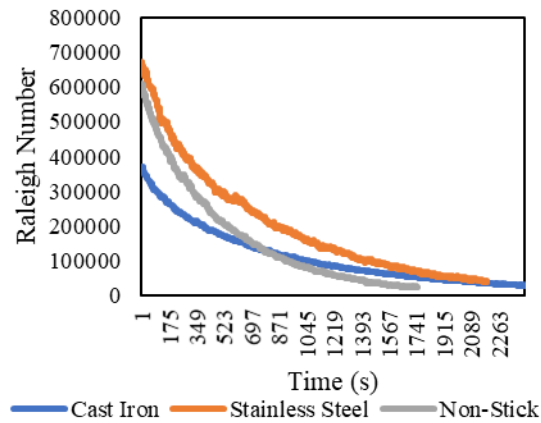


Figure 10. Rayleigh Number vs. Time During Cooling Process

In addition to the individual parts having convection coefficients, the overall system of the pan should have a system convection coefficient. This was calculated using Equation 11 for each pan type and for both conditions. Below in Figure 11 to Figure 16 shows all the convection coefficients calculated over time, for both warming and cooling; Figures 11 and 12 show stainless steel, Figures 13 and 14 show non-stick, and Figures 15 and 16 show cast iron. The average of each of the system convection coefficients can be found in Table 2 after the figures.

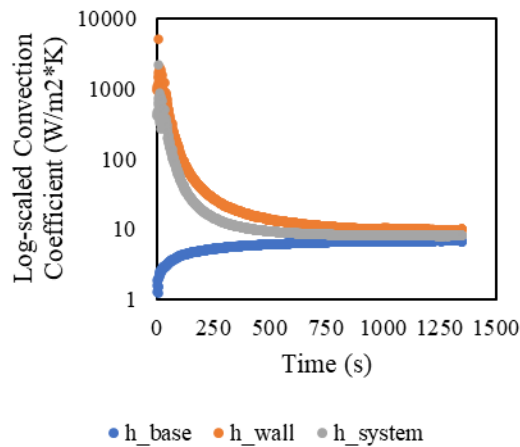


Figure 11. Log-Scaled Convection Coefficients for the Warming Case of Stainless Steel vs Time

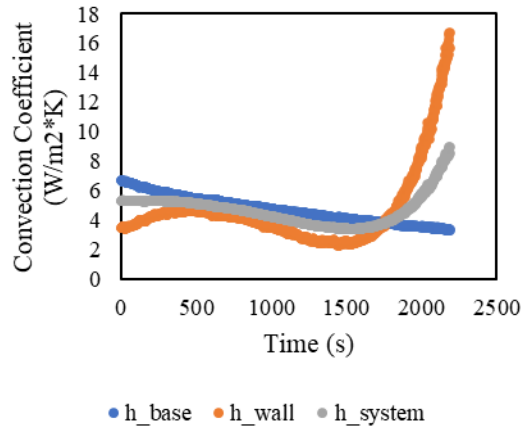


Figure 12. Convection Coefficients for the Cooling Case of Stainless Steel vs Time

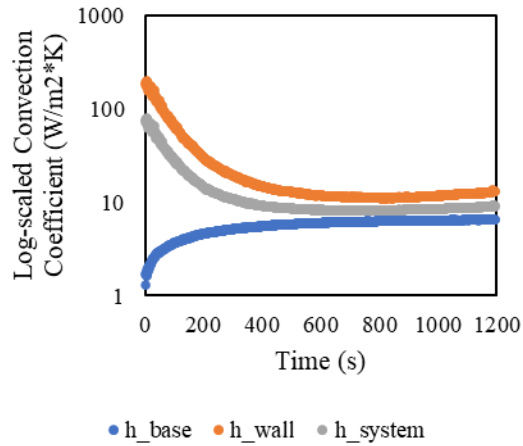


Figure 13. Log-Scaled Convection Coefficients for the Warming Case of Non-Stick vs Time

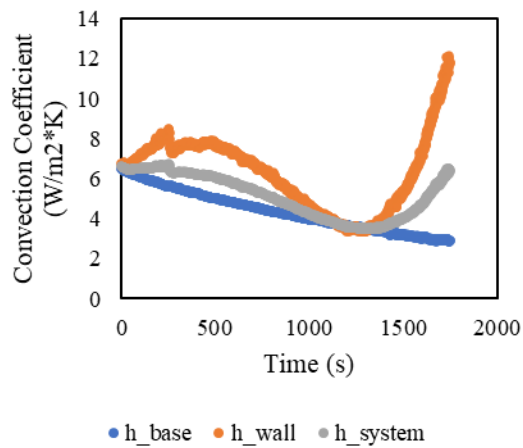


Figure 14. Convection Coefficients for the Cooling Case of Non-Stick vs Time

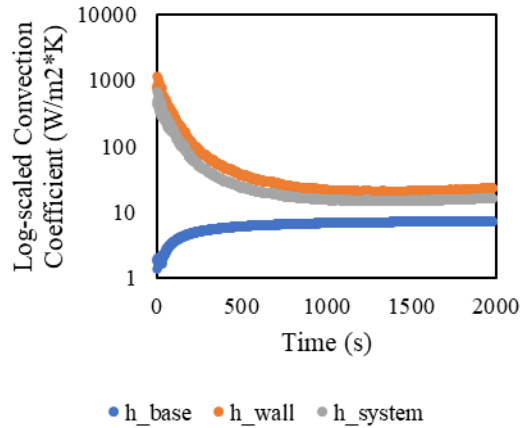


Figure 15. Log-Scaled Convection Coefficients for the Warming Case of Cast Iron vs Time

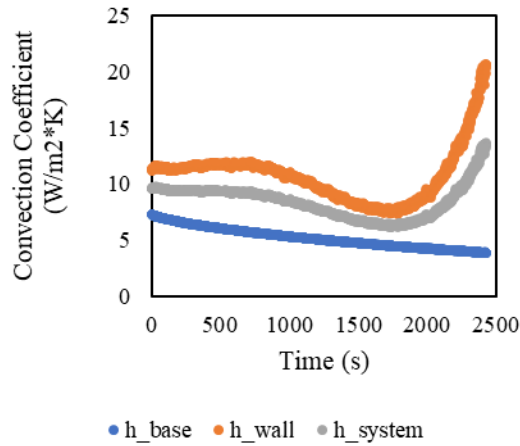


Figure 16. Convection Coefficients for the Cooling Case of Cast Iron vs Time

Table 2. System Convection Coefficient (h_{system}) Average Values

	Stainless Steel	Non-Stick	Cast Iron
h_{system} (W/m ² *K) warming	30.7848	13.2236	37.8220
h_{system} (W/m ² *K) cooling	4.6496	5.1128	8.3843

Some observations from the plots of the convection coefficients over time shows the wall coefficients slightly increasing, then decreasing, then increasing substantially. This could be a result of the walls becoming better convective surfaces, especially as the pan reached steady-state temperature. The convection coefficients for the bases decreased as time went on, which could mean the bases were losing energy via conduction instead of convection.

To determine the accuracy of our data, an uncertainty analysis was done using the Root Mean Square Method. In this method, a best fit plot is compared to actual empirical data to determine how fair from idealistic the collected experimental data was. Our team chose to focus on the Temperature (T) for the uncertainty analysis using the Root Mean Square Error equation below. This value was used as the uncertainty value for the surface temperature at every given time in the later uncertainty analysis.

$$RMSE = \sqrt{\frac{\sum_{i=1}^N (x_i - \bar{x}_i)^2}{N}} \quad (\text{Equation 13})$$

Table 3. Temperature Root Mean Square Errors

	Stainless Steel	Non-Stick	Cast Iron
T (heating) error	0.562344	0.426347	0.717542
T (cooling) error	0.726614	0.432282	0.656815

The following equation was used in order to calculate the error propagation for the Rayleigh number. An example of the work for which can be found in Appendix B. Figures 17-22 highlight the results of the error analysis.

$$\theta_{Ra} = \pm \sqrt{\left(\frac{\delta Ra}{\delta T_s} \theta_{T_s}\right)^2 + \left(\frac{\delta Ra}{\delta T_\infty} \theta_{T_\infty}\right)^2} \quad (\text{Equation 14})$$

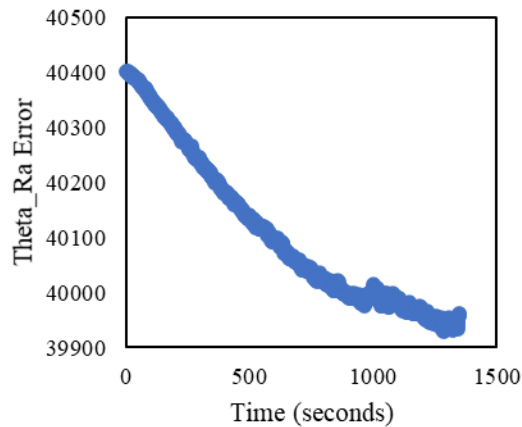


Figure 17. Stainless Steel Warmup Error Propagation for the Rayleigh Number (Ra)

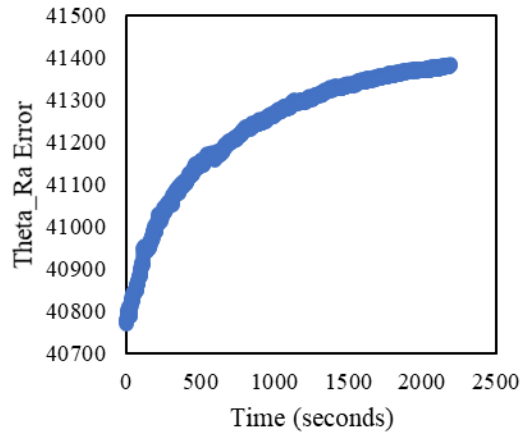


Figure 18. Stainless Steel Cooldown Error Propagation for the Rayleigh Number (Ra).

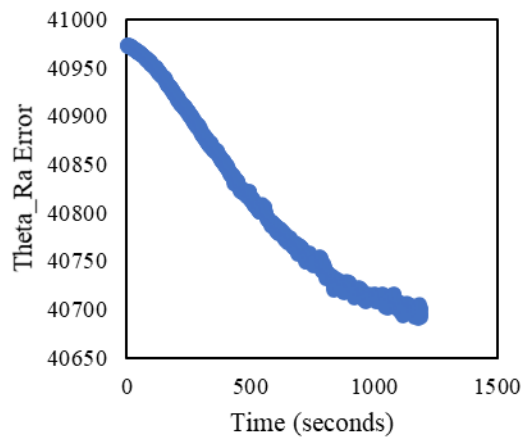


Figure 19. Nonstick Warmup Error Propagation for the Rayleigh Number (Ra).

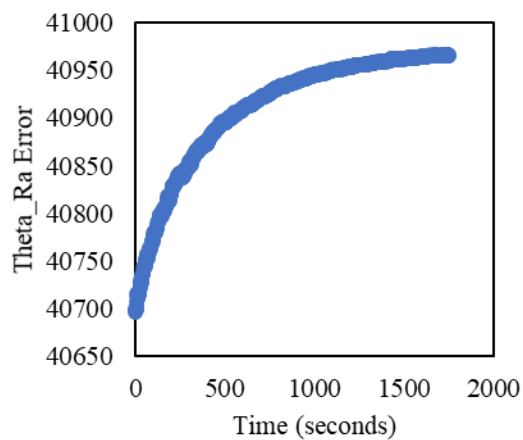


Figure 20. Nonstick Cooldown Error Propagation for the Rayleigh Number (Ra).

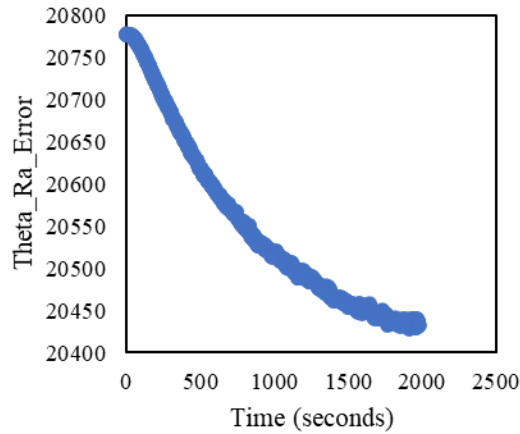


Figure 21. Cast Iron Warmup Error Propagation for the Rayleigh Number (Ra).

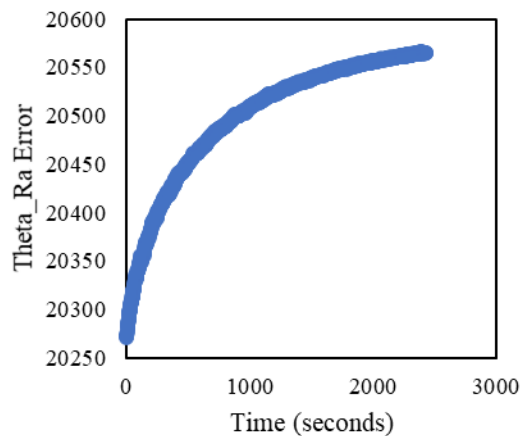


Figure 22. Cast Iron Cooldown Error Propagation for the Rayleigh Number (Ra).

Throughout this experiment there were several notable errors that should be discussed. The first error is the assumption that the top and bottom surfaces of the pans were at uniform temperature. This assumption was made with the primary reason that setting up thermocouples to accurately record temperature on both surfaces would be rather difficult given the restraints of the rest of the experimental set up. Initially, a thermocouple was planned to be placed on the bottom center of the pan to account for this, but there was much difficulty in doing so, so this measurement was abandoned. This was likely the leading cause to the rather high values of the wall convection coefficient in the warming process. Because the surfaces were not at nearly uniform temperatures, conduction should have been taken into account across the pan. However, because that data was not available enough to make an accurate calculation, it was still left out and should be corrected in the future.

The next major error comes from neglecting the handle. In each of the pans, the handle accounts for a large amount of the mass and can likely be considered a large fin extending off the pan and having a large amount of convection occurring on its surface. There is also likely a notable amount of conduction happening through the pan handle as it extends out from the surface of the pan wall. A further expansion of the energy balance equation is needed to take this into account as well as temperature readings at the various points along the handle.

Conclusions and Recommendations

Following the efforts to analyze and compare the heating and cooling properties of different pan materials, this project produced several outcomes in line with theoretical predictions. A few examples of successful discoveries:

- The non-stick pan reached its steady-state temperature the quickest, the cast iron skillet reached the highest steady-state temperature, and the stainless steel pan cooled down from its steady-state temperature the quickest.
- The cast iron skillet exhibited the largest average system convection coefficient values for both heating and cooling, which explains why the longer time period of heating reached a higher steady-state temperature
- The Rayleigh number had an error propagation that was often +/- 20,000 from Ra itself. Since the Rayleigh number was often much larger than 20,000, our team concluded that this is an acceptable propagation of error for both the heating and cooling portions of the experiment.

This project's experimentation and conclusions could be applied to a variety of scenarios in reality. First and foremost, the results can offer an educated decision when purchasing a pan for individual use depending on the culinary application that is targeted. It must be noted that the heating and cooling properties that were detailed in the results section of this report would be significantly more reliable once improvements are implemented into the experimental setup and data acquisition.

Some recommendations for additional experimentation and development of this project can be summarized best by acknowledging the errors of the initial setup. Most importantly, the modified assumptions to account for conduction occurring through the base of the pan and into the

handle from the wall would significantly decrease the values of the wall convection coefficients. In response, an expansion of the energy balance equation to account for conduction into the handle and through the base of the pan would reduce the total error in heat transfer coefficients. Overall, the experiment meet the initial project goal and incorporated various heat transfer fundamentals successfully.

References

Bergman, T. L., Lavine, A., & Incropera, F. P. (2019). *Fundamentals of heat and mass transfer*. John Wiley & Sons, Inc.

Appendix A

Sample Calculation for h_{base} , h_{wall} , and h_{system} During Cooling of the Stainless Steel Pan at
time $t=1s$:

$$Ra = \frac{9.81 \frac{m}{s^2} * \left(\frac{2}{332.67K + 296.25K} \right) * (332.67K - 296.25K) * (.0635m)^3}{1.75 * 10^{-5} \frac{m^2}{s} * 2.49 * 10^{-5} \frac{m^2}{s}} = 667350.758$$

$$Nu = .54 * 667350.758^{\frac{1}{4}} = 15.4341$$

$$h_{base} = \frac{15.4341 * .027494 \frac{W}{mK}}{.0635m} = 6.6826 \frac{W}{m^2K}$$

$$h_{wall} = \frac{-(6.6826 \frac{W}{m^2K} * .050671m^2 * (332.67K - 296.25K)) - (1.3051kg * 475.718 \frac{J}{kgK} * (.5794 * .06671 \frac{K}{s} + .4206 * .05214 \frac{K}{s}))}{13256m^2 * (333.99K - 296.25K)}$$

$$h_{wall} = 3.4398 \frac{W}{m^2K}$$

$$h_{system} = .5794 * 6.6826 \frac{W}{m^2K} + .4206 * 3.4398 \frac{W}{m^2K} = 5.3187 \frac{W}{m^2K}$$

Appendix B

Sample Calculation for Error Propagation:

Cast Iron warmup

Done at $T_s = 30^\circ C$

$T_s = 30 \pm 0.72^\circ C$

$T_\infty = 22 \pm 2^\circ C$

$\theta_{T_s} = 0.72^\circ C$

$\theta_{T_\infty} = 2^\circ C$

$$Ra = \frac{2gL^3}{\alpha\nu} = A (\text{constant}) = \frac{2 \left(9.81 \frac{m^2}{s}\right) (.0505)^3}{(2.4947E - 05)(1.7554E - 05)} = 5770038.572$$

$$\frac{\partial Ra}{\partial T_s} = A \frac{\partial}{\partial T_s} \left(\frac{T_s - T_\infty}{T_s + T_\infty} \right) = \frac{2T_\infty}{(T_s + T_\infty)^2} = \frac{2(295K)}{(303K + 295K)^2} = 9520.5636 \frac{1}{K}$$

$$\frac{\partial Ra}{\partial T_\infty} = A \frac{\partial}{\partial T_\infty} \left(\frac{T_s - T_\infty}{T_s + T_\infty} \right) = - \frac{2T_s}{(T_s + T_\infty)^2} = - \frac{2(303K)}{(303K + 295K)^2} = -9780.2154 \frac{1}{K}$$

$$\theta_{Ra} = \pm \sqrt{\left(\frac{\partial Ra}{\partial T_s} \Big| \theta_{T_s} \right)^2 + \left(\frac{\partial Ra}{\partial T_\infty} \Big| \theta_{T_\infty} \right)^2} \quad (\text{Equation 13})$$

$$\theta_{Ra} = \pm \sqrt{\left(\left(9520.5636 \frac{1}{K} \right) (0.72 K) \right)^2 + \left(\left(9780.2154 \frac{1}{K} \right) (2 K) \right)^2} = 20726.7657$$